Ujjwal Manikya Nath[1] / Chanchal Dey[2] / Rajani K. Mudi[1]

Designing of IMC-PID Controller for Higher-order Process Based on Model Reduction Method and Fractional Coefficient Filter with Real-time Verification

[1] Department of Instrumentation and Electronics Engineering, Jadavpur University, Salt Lake Campus, Kolkata 700098, India, E-mail: um.nath@yahoo.com, rajanikanta.mudi@jadavpuruniversity.in
[2] Department of Applied Physics, Instrumentation Engineering, University of Calcutta, 92 APC Road, Kolkata 700009, India, E-mail: cdaphy@caluniv.ac.in

Abstract:
An improved model reduction scheme is proposed here for higher-order processes and subsequently an enhanced IMC-PID controller is designed based on the obtained reduced model. In the proposed scheme, higher-order processes are estimated as first-order-plus-dead-time (FOPDT) model. Designed IMC controller includes a filter having two separate time constants with fractional order coefficients. Efficacy of the proposed model reduction scheme is verified in terms of closed loop performance evaluation for higher-order minimum and non-minimum phase process models in comparison with improved SIMC (*i*SIMC) controller (Grimholt. Optimal PI and PID control of first-order plus delay processes and evaluation of the original and improved SIMC rules. J Process Control. 2018;70:36–46). Overall performance enhancement for the proposed method is demonstrated through simulation study as well as real-time experimentation on a level control loop.

Keywords: IMC-PID tuning, higher-order process, model reduction, FOPDT process, fractional coefficient filter, real-time level control

DOI: 10.1515/cppm-2019-0089

Received: June 17, 2019; **Revised:** August 20, 2019; **Accepted:** August 26, 2019

1 Introduction

Till date, according to the survey of Desborough and Miller [2] majority of the industrial process loops are found to be managed by PID controller due its simple structure and clear functionality. Among the established tuning methodologies, IMC based PID tuning is being well accepted due to its straightforward designing steps [3]. Primarily, IMC controller for the first-order process model is reported by Rivera *et al.* [4] and later it is extended for second-order process by Chien [5]. Further work on designing of IMC-PID controllers are reported by Morari and Zafiriou [6]. Literature survey reveals that IMC controllers are quite competent to provide good set point response [7] but they usually offer sluggish load recovery [1, 7, 8], especially for lag dominating processes.

To enhance load regulation, Skogestad proposed an IMC tuning scheme known as SIMC [7] where the integral time is intentionally made smaller for lag dominating processes and similar approach is also reported by Lee et al. [8]. Performance of the SIMC controller has been further improved (*i*SIMC) by incorporating a derivative term in the controller structure as reported by Grimholt and Skogestad [1]. However, during IMC designing, proper choice of the closed loop time constant (λ) plays a very vital role towards ensuring desirable closed loop response. To obtain a suitable value of λ, straight forward guideline can be found in [1, 7, 8] for first-order plus time delay (FOPDT) and second-order plus time delay (SOPDT) processes. As previously discussed, in most of the cases [7, 8] *tight tuning* scheme is favored for IMC controller to achieve good load recovery. However, *smooth tuning* technique is also preferable for industrial processes during set point tracking [9]. To choose a controller behavior (*smooth* or *tight*), maximum sensitivity (M_s) [10] plays a very important role. An IMC controller may also be tuned based on maximum sensitivity method as reported in [11, 12]. In [11], guideline is provided to calculate λ based on maximum sensitivity for *smooth* and *tight* control strategies. Designing of an optimal IMC controller is found in [1, 13]. Moreover, works reported in [14–18] discuss about the other approaches of IMC controller designing.

Ujjwal Manikya Nath is the corresponding author.

In practice, as the actual processes are of higher-order [19] so it is not easy to design IMC controller for them unless they are approximated in FOPDT or SOPDT form [20]. Half rule method [7] is an effective model reduction technique to obtain FOPDT or SOPDT structure from higher-order models. Another refined version of half rule method is reported by Lee *et al.* [8]. Here, initially an analytical discussion on the proposed model reduction technique to obtain FOPDT model from higher-order processes is provided. Based on the open loop process responses it is found that the reduced model obtained by the proposed technique shows closeness with the actual model than that of the conventional half rule [7] method. Subsequently, IMC based PID controller is designed where the chosen filter has two distinct fractional-order time constants. Guidelines are provided for the selection of time constants based on maximum sensitivity. Presence of fractional-order time constants provides additional flexibility towards the choice of controller with *tight* or *smooth* or optimal behavior. For simulation study, higher-order minimum and non-minimum phase process models are considered. Closed loop performance evaluation is made with *i*SIMC settings reported in literature [1]. In addition to extensive simulation study, superiority of the proposed scheme is also verified through real-time implementation on a level control loop [21].

In Section 2, discussion is provided on problem formulation along with analytical discussion on proposed model reduction technique. Proposed controller designing methodology is reported in Section 3. Simulation study along with real-time experimentation on a level control loop is discussed in Section 4. At the end, conclusion is provided in Section 5.

2 Problem formulation with proposed model reduction technique

Considering a higher-order process as given by eq. (1)

$$G_P(s) = \frac{k_p\left(\beta_m s^m + \beta_{m-1}s^{m-1} + \ldots\ \ldots\ \ldots\ \ldots\ \beta_0\right)}{\alpha_n s^n + \alpha_{n-1}s^{n-1} + \ldots\ \ldots\ \ldots\ \ldots\ \alpha_n} e^{-\theta s} \tag{1}$$

where $n > m$. Here, we consider that the process model has i number of right hand plane (RHP) zeros as represented by eq. (2).

$$G_P(s) = \frac{k_p\left(-T_i s+1\right)\left(-T_{i-1}s+1\right)\ \ldots\ \ldots\ \ldots\ \ldots\ \left(-T_1 s+1\right)\left(\delta_j s+1\right)\left(\delta_{j-1}s+1\right)\ \ldots\ \ldots\ \ldots\ \ldots\ \left(\delta_1 s+1\right)}{\left(\tau_n s+1\right)\left(\tau_{n-1}s+1\right)\ \ldots\ \ldots\ \ldots\ \ldots\ \left(\tau_1 s+1\right)} e^{-\theta s} \tag{2}$$

where $m = i + j$.

Dead time part of eq. (2) is approximated by first-order Pade's approximation and can be expressed as

$$G_P(s) = \frac{k_p\left(-T_i s+1\right)\left(-T_{i-1}s+1\right)\ \ldots\ \ldots\ \ldots\ \ldots\ \left(-T_1 s+1\right)\left(\delta_j s+1\right)\left(\delta_{j-1}s+1\right)\ \ldots\ \ldots\ \ldots\ \ldots\ \left(\delta_1 s+1\right)}{\left(\tau_n s+1\right)\left(\tau_{n-1}s+1\right)\ \ldots\ \ldots\ \ldots\ \ldots\ \left(\tau_1 s+1\right)} \frac{-0.5\theta s+1}{0.5\theta s+1}. \tag{3}$$

Now, it is not feasible to realize PID controller from the higher-order relation as given by eq. (3) and hence it is approximated as FOPDT form using the proposed model reduction technique. A general expression of higher-order process with RHP zero is considered as

$$G_p(s) = \frac{k_p \prod_i \left(-T_i s+1\right)}{\prod_n \left(\tau_n s+1\right)} e^{-\theta s}. \tag{4}$$

Now, considering the case $\tau_1 > \tau_2 > \tau_3 > \cdots > \tau_n$ and $T_1 > T_2 > T_3 > \cdots > T_i$. eq. (4) can be expressed as

$$G_P(s) = \frac{k_p\left(-T_i s+1\right)\left(-T_{i-1}s+1\right)\ \ldots\ \ldots\ \ldots\ \ldots\ \left(-T_1 s+1\right)}{\left(\tau_n s+1\right)\left(\tau_{n-1}s+1\right)\ \ldots\ \ldots\ \ldots\ \ldots\ \left(\tau_1 s+1\right)} e^{-\theta s}. \tag{5}$$

By Taylor series approximation $-T_i s + 1$, $-T_{i-1}s + 1$, and $-T_1 s + 1$ can be written as $e^{-T_i s} e^{-T_{i-1}s}$ and $e^{-T_1 s}$ respectively and eq. (5) can be represented by following relation

$$G_P(s) = \frac{k_p}{\left(\tau_n s+1\right)\left(\tau_{n-1}s+1\right)\ \ldots\ \ldots\ \ldots\ \ldots\ \left(\tau_1 s+1\right)} e^{-\left(T_i+T_{i-1}+\ \ldots\ +T_1+\theta\right)s}. \tag{6}$$

Denominator part of eq. (6) is

$$(\tau_n s + 1)(\tau_{n-1} s + 1) \ldots \ldots \ldots \ldots (\tau_1 s + 1). \tag{7}$$

Ignoring coefficients of the higher-order s terms (s^n, $s^{n-1} \ldots s^3$) as $\tau_n < \tau_{n-1} < \ldots \tau_2 < \tau_1$ eq. (7) can be represented as

$$\tau_n s + \tau_{n-1} s + \ldots \tau_3 s + + \tau_2 s + \tau_1 s + \tau_1 \tau_2 s^2 + 1$$

$$= \tau_1 \tau_2 s^2 + \tau_1 s + \tau_2 s + 1 + \tau_3 s + \tau_{n-1} s + \ldots \tau_n s$$

$$= \left[\frac{\tau_1^2 + 2\tau_1 \frac{\tau_2}{2} + \left(\frac{\tau_2}{2}\right)^2}{2} s^2 + \left(\tau_1 + \frac{\tau_2}{2}\right) s + 1\right] - \left[\frac{\tau_1^2 + \frac{\tau_2^2}{4}}{2} s^2 + \left(\sqrt{\tau_1^2 + \frac{\tau_2^2}{4}}\right) s + 1\right] +$$
$$\left[\frac{\tau_1 \tau_2}{2} s^2 + \sqrt{\tau_1 \tau_2} s + 1\right] - \left[\sqrt{\tau_1 \tau_2} s + 1\right] + \left[\left(\frac{\tau_2}{2} + \sqrt{\tau_1^2 + \frac{\tau_2^2}{4}}\right) s + 1\right] + \tau_3 s + \tau_{n-1} s + \ldots \tau_n s$$

$$= e^{\left(\tau_1 + \frac{\tau_2}{2}\right) s} - e^{\sqrt{\tau_1^2 + \frac{\tau_2^2}{2}} s} + e^{\sqrt{\tau_1 \tau_2} s} - e^{\sqrt{\tau_1 \tau_2} s} + e^{\left(\frac{\tau_2}{2} + \sqrt{\tau_1^2 + \frac{\tau_2^2}{4}}\right) s} + \tau_3 s + \tau_{n-1} s + \ldots \tau_n s. \tag{8}$$

Considering up to 1st s terms of Taylor series from eq. (8)

$$= \left[\left(\tau_1 + \frac{\tau_2}{2}\right) s + 1\right] - \left[\left(\sqrt{\tau_1^2 + \frac{\tau_2^2}{4}}\right) s + 1\right] + \left[\left(\frac{\tau_2}{2} + \sqrt{\tau_1^2 + \frac{\tau_2^2}{4}}\right) s + 1\right] + \tau_3 s + \tau_{n-1} s + \ldots \tau_n s. \tag{9}$$

Now, simplifying eq. (9), we get

$$= \left(\tau_1 + \frac{\tau_2}{2}\right) s - \left(\sqrt{\tau_1^2 + \frac{\tau_2^2}{4}}\right) s + \left(\frac{\tau_2}{2} + \sqrt{\tau_1^2 + \frac{\tau_2^2}{4}}\right) s + 1 + \tau_3 s + \tau_{n-1} s + \ldots \tau_n s$$

$$= \underbrace{\left(\tau_1 + \frac{\tau_2}{2} - \sqrt{\tau_1^2 + \frac{\tau_2^2}{4}} + \tau_3 + \tau_{n-1} + \ldots \tau_n\right)}_{\theta_{approx}} s + \underbrace{\left(\frac{\tau_2}{2} + \sqrt{\tau_1^2 + \frac{\tau_2^2}{4}}\right)}_{\tau_{approx}} s + 1. \tag{10}$$

Using eq. (10), eq. (6) can be written as

$$\tilde{G}_p(s) = \frac{k_p}{(\tau_{approx} s + 1)} e^{-\left(\theta_{approx} + T_i + T_{i-1} + \ldots + T_1 + \theta\right) s}. \tag{11}$$

Equation (11) has two parts $\theta_{reduced}$ and $\tau_{reduced}$ as given by eq. (12) and eq. (13) respectively

$$\theta_{reduced} = \theta_{approx} + T_i + T_{i-1} + \ldots + T_1 + \theta., \tag{12}$$

$$\tau_{reduced} = \tau_{approx}. \tag{13}$$

Now, eqs. (12) and (13) can be written as

$$\theta_{reduced} = \tau_1 + \frac{\tau_2}{2} - \sqrt{\tau_1^2 + \frac{\tau_2^2}{4}} + \tau_3 + \tau_{n-1} + \ldots \tau_n + T_i + T_{i-1} + \ldots T_1 + \theta, \tag{14}$$

$$\tau_{reduced} = \frac{\tau_2}{2} + \sqrt{\tau_1^2 + \frac{\tau_2^2}{4}}. \tag{15}$$

Now, from eq. (14) we get

$$\begin{aligned}
\theta_{reduced} &= \tau_1 + \frac{\tau_2}{2} - \sqrt{\tau_1^2 + \frac{\tau_2^2}{4}} + \tau_3 + \tau_{n-1} + \ \ldots\ \tau_n + T_i + T_{i-1} + \ \ldots\ T_1 + \theta \\
&= \tau_1\left[1 + \frac{\tau_2}{2\tau_1} - \sqrt{1 + \left(\frac{\tau_2}{2\tau_1}\right)^2}\right] + \tau_3 + \tau_{n-1} + \ \ldots\ \tau_n + T_i + T_{i-1} + \ \ldots\ T_1 + \theta \\
&\approx \tau_1\left[1 + \frac{\tau_2}{2\tau_1} - \left(1 + 0.5\frac{\tau_2{}^2}{4\tau_1{}^2}\right)\right] + \tau_3 + \tau_{n-1} + \ \ldots\ \tau_n + T_i + T_{i-1} + \ \ldots\ T_1 + \theta \\
&= \frac{\tau_2}{2} - \frac{\tau_2^2}{8\tau_1} + \tau_3 + \tau_{n-1} + \ \ldots\ \tau_n + T_i + T_{i-1} + \ \ldots\ T_1 + \theta \\
\text{i. e. } \theta_{reduced} &= 0.5\tau_2\left(1 - \frac{\tau_2}{4\tau_1}\right) + \tau_3 + \tau_{n-1} + \ldots \tau_n + T_i + T_{i-1} + \ldots T_1 + \theta. \qquad (16)
\end{aligned}$$

Similarly, from eq. (15) we get

$$\tau_{reduced} = \frac{\tau_2}{2} + \sqrt{\tau_1^2 + \frac{\tau_2^2}{4}}$$

$$= \frac{\tau_2}{2} + \tau_1\left[1 + \left(\frac{\tau_2}{2\tau_1}\right)^2\right]^{1/2}$$

$$\approx \frac{\tau_2}{2} + \tau_1\left[1 + 0.5\left(\frac{\tau_2}{2\tau_1}\right)^2\right]$$

$$= \frac{\tau_2}{2} + \tau_1 + \frac{\tau_2^2}{8\tau_1}$$

$$\text{i.e., } \tau_{reduced} = \tau_1 + 0.5\tau_2\left(1 + \frac{\tau_2}{4\tau_1}\right). \qquad (17)$$

For higher-order process as given by eq. (4), $\tau_{reduced}$ and $\theta_{reduced}$ can be expressed by eq. (18) and eq. (19) respectively.

$$\tau_{reduced} \approx \tau_1 + 0.5\tau_2\left(1 + \frac{\tau_2}{4\tau_1}\right), \qquad (18)$$

$$\theta_{reduced} \approx \theta + 0.5\tau_2\left(1 - \frac{\tau_2}{4\tau_1}\right) + \sum\nolimits_{n\geqslant 3}\tau_n + \sum\nolimits_i T_i. \qquad (19)$$

In the subsequent section we will discuss about the proposed model reduction scheme for a second-order plus dead process with right hand plane zero as given by eq. (20)

$$G_1(s) = \frac{-T_1 s + 1}{(\tau_1 s + 1)(\tau_2 s + 1)} e^{-\theta s}. \qquad (20)$$

Here, $(-T_1 s + 1)$ is approximated as Tayor series expansion and eq. (20) is written as

$$G_1(s) = \frac{1}{(\tau_1 s + 1)(\tau_2 s + 1)} e^{-(T_1 + \theta)s}. \qquad (21)$$

Denominator of eq. (21) can be represented by

$$(\tau_1 s+1)(\tau_2 s+1) = \tau_1\tau_2 s^2 + (\tau_1+\tau_2)s + 1$$

$$= \underbrace{\left(\tau_1 + \frac{\tau_2}{2} - \sqrt{\tau_1^2 + \frac{\tau_2^2}{4}}\right)}_{\theta_{approx}} S + \underbrace{\left(\frac{\tau_2}{2} + \sqrt{\tau_1^2 + \frac{\tau_2^2}{4}}\right)}_{\tau_{approx}} S + 1. \tag{22}$$

Equation (22) can be written as

$$\tilde{G}_1(s) = \frac{1}{(\tau_{approx}s+1)} e^{-\left(\theta_{approx}+T_1+\theta\right)s}. \tag{23}$$

Equation (23) has two parts $\theta_{reduced}$ and $\tau_{reduced}$ as given by eq. (24) and eq. (25) respectively

$$\tau_{reduced} \approx \tau_1 + 0.5\tau_2\left(1 + \frac{\tau_2}{4\tau_1}\right), \tag{24}$$

$$\theta_{reduced} \approx \theta + 0.5\tau_2\left(1 - \frac{\tau_2}{4\tau_1}\right) + T_1. \tag{25}$$

To justify the effectiveness of our proposed model reduction scheme, open loop step responses are studied with the reduced FOPTD model along with the actual higher-order process. For the quantitative estimation of model mismatch between the true higher-order process and its reduced model, integral absolute error (IAE) is calculated based on the difference of responses of the actual higher-order process and its reduced FOPDT model. Figure 1 shows the block diagram of the aforesaid experimentation scheme where a unit step input is simultaneously applied to the actual higher-order process along with its reduced FOPTD model and corresponding IAE values are listed in Table 1. Proposed model reduction technique provides lesser IAE value compared to the half rule [7] based reduced model. However, frequency domain analysis is also performed through Bode plot as shown in Figure 2. Graphical results reveal that the proposed reduced FOPDT model provides somewhat closer gain and phase varying behavior with respect to the actual higher-order process compared to the half rule based FOPDT model.

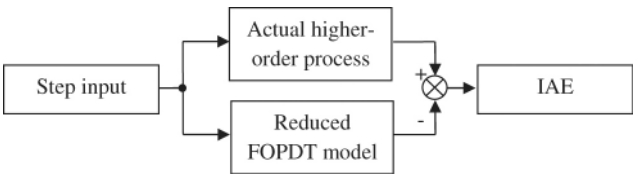

Figure 1: Comparison between the actual higher-order model and its equivalent FOPDT form in terms of IAE values computed from the difference of responses under unit step input.

Table 1: Actual higher-order model, corresponding reduced FOPDT form and their respective IAE values.

Higher-order model	Approximated FOPDT model		IAE	
	Half rule [7]	Proposed	Half rule [7]	Proposed
$\frac{1}{(1+s)^4}$ [7, 17, 18]	$\frac{1}{(1.5s+1)}e^{-2.5s}$	$\frac{1}{(1.625s+1)}e^{-2.375s}$	0.511	0.436
$\frac{(-2s+1)}{(s+1)^3}$ [7, 17, 18]	$\frac{1}{(1.5s+1)}e^{-3.5s}$	$\frac{1}{(1.625s+1)}e^{-3.375s}$	1.006	1.005
$\frac{(-s+1)}{(s+1)^5}e^{-2s}$ [18]	$\frac{1}{(1.5s+1)}e^{-6.5s}$	$\frac{1}{(1.625s+1)}e^{-6.375s}$	1.067	0.55

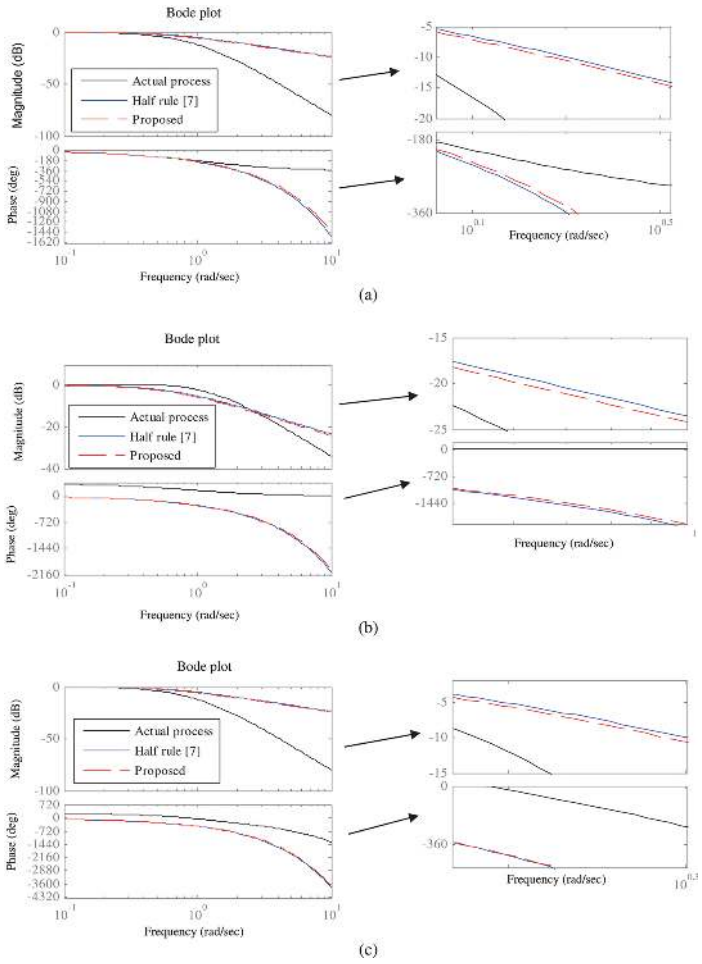

Figure 2: Bode plot for (a) $\frac{1}{(1+s)^4}$ (b) $\frac{(-2s+1)}{(s+1)^3}$ and (c) $\frac{(-s+1)}{(s+1)^5}e^{-2s}$.

3 Proposed IMC-PID tuning

Block diagram of IMC control technique [4–6, 9, 11] is shown in Figure 3. Basic structure of IMC based control loop and its equivalent feedback form is shown in Figure 4. By solving the inner loop of Figure 4 we get the controller structure and the IMC-PID controller can be given by

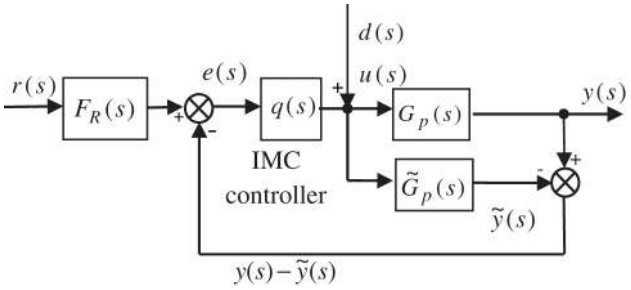

Figure 3: Block diagram of IMC structure.

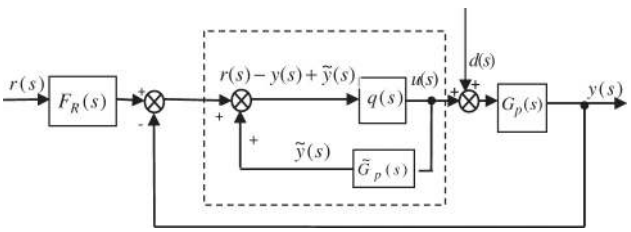

Figure 4: IMC equivalent feedback structure.
G_p = process
$\tilde{G}_p$ = process model
q = internal model controller
$\tilde{y}$ = model output
F_R = set point filter
r = set point
e = error = $r - y + \tilde{y}$
d = load disturbance
u = manipulated input (controller output)
y = measured process output

$$G_c(s) = \frac{q(s)}{1 - \tilde{G}_p(s)\, q(s)}. \tag{26}$$

Substituting the value of individual terms in eq. (26) and comparing with the expression of non-interacting PID controller (eq. (27)) we get the PID tuning parameters, i. e. the values of k_c, τ_I, and τ_D. In general, this methodology results in an ideal form of PID (i. e. parallel or non-interacting) controller cascaded with a first-order noise filter (with time constant τ_F) as given by

$$G_c(s) = k_c \left[\frac{\tau_I \tau_D s^2 + \tau_I s + 1}{\tau_I s}\right]\left[\frac{1}{\tau_F s + 1}\right]. \tag{27}$$

In the present work, higher-order industrial processes are reduced to FOPDT form as given by $\tilde{G}_p(s) = \frac{k_p e^{-\theta_{reduced} s}}{(\tau_{reduced} s + 1)}$. Designing of IMC-PID controller for FOPDT model can be described by the following steps –

Step I: Process delay is realized by first-order *Pade's* approximation $\tilde{G}_p(s) = \frac{k_p}{(\tau_{approx} s + 1)} \frac{(-0.5\theta_{reduced} s + 1)}{(0.5\theta_{reduced} s + 1)}$.

Step II: FOPDT model is factorized into invertible and non-invertible parts

$$\tilde{G}_p(s) = \tilde{G}_{p+}(s)\, \tilde{G}_{p-}(s) = \left[\frac{k_p}{(\tau_{reduced} s + 1)(0.5\theta_{reduced} s + 1)}\right](-0.5\theta_{reduced} s + 1).$$

Step III: Model inversion is done for the invertible part of $\tilde{G}_p(s)$

$$\tilde{q}(s) = \tilde{G}_{p+}^{-1}(s) = \frac{(\tau_{reduced} s + 1)(0.5\theta_{reduced} s + 1)}{k_p}.$$

Step IV: According to the proposed scheme a fractional coefficient filter with two different time constants $\lambda_1^{\gamma_1}$ and $\lambda_2^{\gamma_2}$ is added in series with $\tilde{q}(s)$ and the resulting controller structure will be

$$q(s) = \tilde{q}(s) f(s) = \tilde{G}_{p+}^{-1}(s) f(s) = \frac{(\tau_p s + 1)(0.5\theta s + 1)}{k_p} \frac{1}{(\lambda_1^{\gamma_1} s + 1)(\lambda_2^{\gamma_2} s + 1)},$$

where γ_1 and γ_2 are fractional values.

Step V: By solving eq. (26) and comparing with the expression of non-interacting PID controller (eq. (27)), tuning parameters of IMC-PID controller can be given by

$$k_c = \frac{\tau_{reduced} + 0.5\theta_{reduced}}{k_p(\lambda_1^{\gamma_1} + \lambda_2^{\gamma_2} + 0.5\theta_{reduced})}, \tag{28}$$

$$\tau_I = \tau_{reduced} + 0.5\theta_{reduced}, \tag{29}$$

$$\tau_D = \frac{\tau_{reduced}\theta_{reduced}}{2\tau_{reduced} + \theta_{reduced}}, \tag{30}$$

$$\tau_F = \frac{\lambda_1^{\gamma_1}\lambda_2^{\gamma_2}}{\lambda_1^{\gamma_1} + \lambda_2^{\gamma_2} + 0.5\theta_{reduced}}. \tag{31}$$

Now, substituting the values of $\tau_{reduced}$ and $\theta_{reduced}$ from eq. (18) and eq. (19) in the eqs. (28)–(31), tuning parameters of the PID controller will be given by

$$k_c = \frac{\left[\tau_1 + 0.5\tau_2\left(1+\frac{\tau_2}{4\tau_1}\right)\right] + 0.5\left[\theta + 0.5\tau_2\left(1-\frac{\tau_2}{4\tau_1}\right) + \sum_{n\geqslant 3}\tau_n + \sum_i T_i\right]}{k_p\left[\lambda_1^{\gamma_1} + \lambda_2^{\gamma_2} + 0.5\left\{\theta + 0.5\tau_2\left(1-\frac{\tau_2}{4\tau_1}\right) + \sum_{n\geqslant 3}\tau_n + \sum_i T_i\right\}\right]}, \tag{32}$$

$$\tau_I = \tau_1 + 0.5\tau_2\left(1+\frac{\tau_2}{4\tau_1}\right) + 0.5\left[\theta + 0.5\tau_2\left(1-\frac{\tau_2}{4\tau_1}\right) + \sum_{n\geqslant 3}\tau_n + \sum_i T_i\right], \tag{33}$$

$$\tau_D = \frac{\left[\tau_1 + 0.5\tau_2\left(1+\frac{\tau_2}{4\tau_1}\right)\right]\left[\theta + 0.5\tau_2\left(1-\frac{\tau_2}{4\tau_1}\right) + \sum_{n\geqslant 3}\tau_n + \sum_i T_i\right]}{2\left[\tau_1 + 0.5\tau_2\left(1+\frac{\tau_2}{4\tau_1}\right)\right] + \left[\theta + 0.5\tau_2\left(1-\frac{\tau_2}{4\tau_1}\right) + \sum_{n\geqslant 3}\tau_n + \sum_i T_i\right]}, \tag{34}$$

$$\tau_F = \frac{\lambda_1^{\gamma_1}\lambda_2^{\gamma_2}}{\lambda_1^{\gamma_1} + \lambda_2^{\gamma_2} + 0.5\left[\theta + 0.5\tau_2\left(1-\frac{\tau_2}{4\tau_1}\right) + \sum_{n\geqslant 3}\tau_n + \sum_i T_i\right]}. \tag{35}$$

Tuning parameters λ_1 and λ_2 in the eqs. (32)–(35) are required to be provided and they may be calculated based on Maximum sensitivity (M_s) method as described by Ali and Majhi [11]. Typical range of M_s is 1.2 to 2.0 [10] where the lower value of M_s indicates robust behavior of the controller, alternatively the higher value of M_s provides *tight* behavior during closed loop performance. As reported in [11], the relation between λ and M_s can be written as

$$\lambda = \left(\frac{2 + 2\sqrt{1-c} - c - 2c^2}{2c^2}\right)\theta \tag{36}$$

where $c = \sqrt{1 - \frac{1}{M_s^2}}$.

Now, the two tuning parameters $\lambda_1$and λ_2 can be obtained from eq. (36). λ_1 is calculated for $M_s = 1.2$ (to accomplish robust behaviour) whereas the value of λ_2 is obtained for $M_s = 2.0$ (*tight* control mode). Accordingly, the values for λ_1 and λ_2 are provided by eq. (37).

$$\lambda_1 = 3.556\theta \text{ and } \lambda_2 = 0.244\theta. \tag{37}$$

Now, two other tuning parameters with fractional values γ_1 and γ_2 are required to be chosen. To study the effect of the fractional parameters (γ_1 and γ_2), a typical higher-order process model $\left(G_p(s) = \frac{1}{(1+s)^4}\right)$ [7, 17, 18] is selected from the literature. Performance of the proposed controller is tested for different combinations of γ_1 and γ_2 which are listed in Table 2. For different rational values of γ_1 and γ_2, i. e. ($0 \leqslant \gamma_1 \leqslant 1$, $0 \leqslant \gamma_2 \leqslant 1$), ($1 \leqslant \gamma_1 \leqslant 2$, $1 \leqslant \gamma_2 \leqslant 2$) and irrational values of γ_1 and γ_2, i. e. ($\gamma_1 = \sqrt{0.5}$, $\gamma_2 = \sqrt{0.5}$) and ($\gamma_1 = \sqrt{1.5}$, $\gamma_2 = \sqrt{1.5}$), corresponding closed loop responses are shown in Figure 5. It depicts that the choice $\gamma_1 = 1$,$\gamma_2 = 0$ provides sluggish process response with a lower M_s value ($M_s = 1.15$). Whereas $\gamma_1 = 0$, $\gamma_2 = 1$ provides aggressive control performance with a higher value of M_s ($M_s = 1.47$), which substantiates relatively poor robustness of the controller. However, good set point response (minimum overshoot as well as faster tracking) with acceptable load recovery (when a step load disturbance is introduced) can be achieved with the selection of $\gamma_1 = 0.5$, $\gamma_2 = 0.5$ with $M_s = 1.299$.

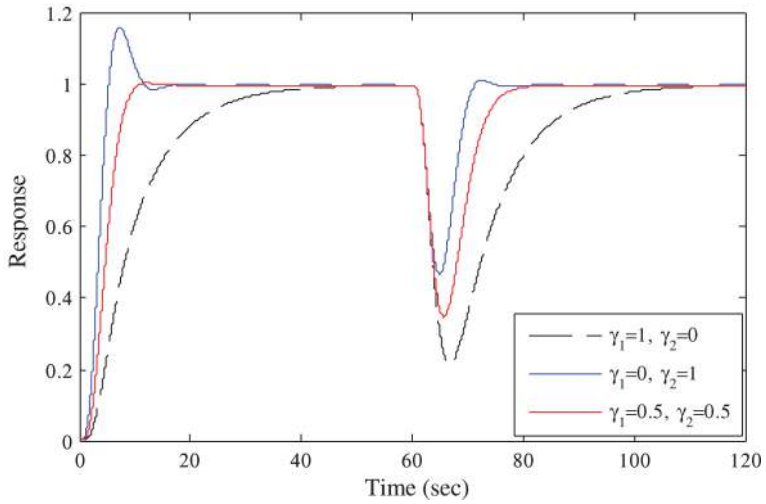

Figure 5: Effects of γ_1 and γ_2 ($0 \leqslant \gamma_1 \leqslant 1, 0 \leqslant \gamma_2 \leqslant 1$) during closed loop performance for the process model $\frac{1}{(1+s)^4}$.

Table 2: Effects of γ_1 and γ_2 in controller tuning parameters.

Model	Fractional coefficients		IAE		M_S
	γ_1	γ_2	Set point tracking	Load rejection	
$\frac{1}{(1+s)^4}$ [7, 17, 18]	1	0	10.63	10.63	1.15
	0	1	3.97	2.83	1.47
	0.5	0.5	4.89	4.85	1.29
	1	1	10.20	10.21	1.14
	2	0	41.81	57.99	1.03
	0	2	3.823	2.589	1.48
	$\sqrt{0.5}$	$\sqrt{0.5}$	6.388	6.388	1.22
	$\sqrt{1.5}$	$\sqrt{1.5}$	15.16	15.44	1.09

4 Results

Performance assessment of the proposed scheme is performed through simulation study as well as real-time experimentation on a level control loop. For simulation study, both minimum phase and non-minimum phase higher-order process models are considered. Performance of our proposed model reduction based IMC-PID controller is compared with *i*SIMC controller [1] in terms of integral absolute error (IAE) = $\int_0^\infty e(t)dt$ and total variation (TV) in control action= $\sum_{k=1}^{\infty} |u_{k+1} - u_k|$ (control action is considered as a discretized sequence $u_1, u_2, u_3 \ldots u_{k\ldots}$) during set point tracking and load recovery phases. For robustness study, the maximum sensitivity $M_s = max\left|\frac{1}{1+G_pG_c}\right|$ is also computed for each case. During real-time verification on a level control loop, IAE and TV values are also computed for the proposed controller along with well-known IMC settings [1]. From both the simulation study and real-time experimental results it is observed that an overall acceptable performance is provided by our proposed IMC-PID controller.

The tuning relation of *i*SIMC [1] controller is given by

$$k_c' = \frac{\tau_{half\ rule}}{k_p\left(\lambda + \theta_{half\ rule}\right)}, \tag{38}$$

$$\tau_I' = \min\left\{\tau_{half\ rule},\ 4\left(\lambda + \theta_{half\ rule}\right)\right\}, \tag{39}$$

$$\tau_D' = \theta_{half\ rule}/3. \tag{40}$$

where $\lambda = \theta$.

However, eqs. (38)–(40) represent tuning parameters for series PID form [1]. The corresponding expression of tuning parameters for parallel PID form are given by

$$k_c = k_c' f, \tau_I = \tau_I' f, \text{ and } \tau_D = \tau_D'/f \text{ where } f = \left(1 + \frac{\tau_D'}{\tau_I'}\right). \tag{41}$$

4.1 Simulation study

Model I: $\frac{1}{(1+s)^4}$

This minimum phase fourth-order process model [7, 17, 18] is approximated as FOPDT model using half rule method [7] as well as our proposed technique and they are given by $\frac{1}{(1.5s+1)}e^{-2.5s}$ and $\frac{1}{(1.625s+1)}e^{-2.375s}$ respectively. Tuning parameters for half rule based FOPDT model are calculated using *i*SIMC [1] guideline and its performance is compared with the suggested tuning based on the proposed reduced model. For the proposed case, $\lambda_1 = 8.44$ and $\lambda_2 = 0.579$ (based on eq. (37)) with $\gamma_1 = \gamma_2 = 0.5$. During closed loop operation the related performance indices are listed in Table 3 and the process response is shown in Figure 6. The proposed method provides lesser IAE values during set point tracking as well as load recovery phases.

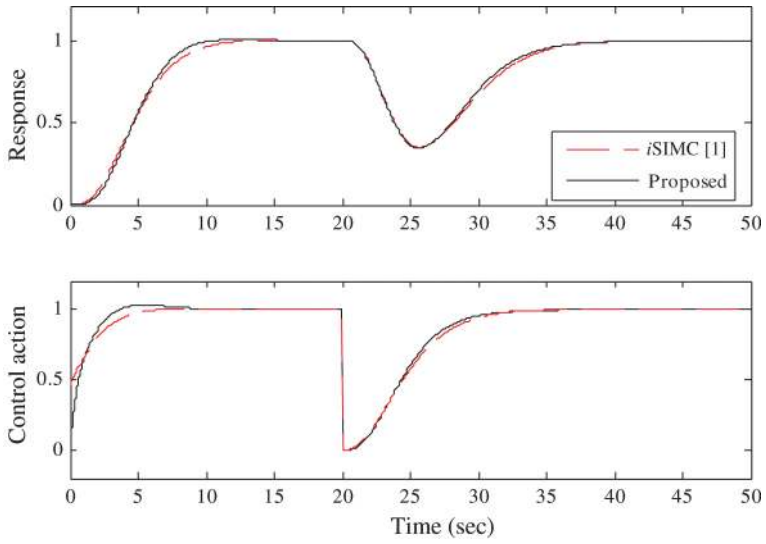

Figure 6: Closed loop responses for model I.

Table 3: Simulation results.

Model Tuning		Controller parameter				Set point tracking		Load rejection		M_s
		k_c	τ_I	τ_I	τ_F	IAE	TV	IAE	TV	
I	*i*SIMC [1]	0.467	2.333	0.535	–	5.01	1.01	4.99	1.02	1.238
	Proposed	0.579	2.812	0.686	0.455	4.89	1.05	4.85	0.98	1.299
II	*i*SIMC [1]	0.381	2.667	0.6563	–	6.99	0.99	8.16	1.42	1.501
	Proposed	0.546	3.312	0.827	0.518	6.06	1.26	7.27	1.52	1.912
III	*i*SIMC [1]	0.281	3.667	0.885	–	13.04	0.99	13.15	1.03	1.373
	Proposed	0.523	4.812	1.076	0.645	10.09	1.32	9.29	1.15	1.751

Model II: $\frac{(-2s+1)}{(s+1)^3}$

This non-minimum phase higher-order process model is chosen from [7, 17, 18]. Approximated FOPDT models based on half rule method [7] as well as the proposed technique are given by $\frac{1}{(1.5s+1)}e^{-3.5s}$ and $\frac{1}{(1.625s+1)}e^{-3.375s}$ respectively. The proposed setting is compared with a recently published work by Grimholt and Skogestad [1] where the tuning relations are given in eqs. (38)–(40) and the corresponding non-interacting form of PID tuning parameters are calculated according to eq. (41). Here, $\lambda_1 = 12$ and $\lambda_2 = 0.823$ with $\gamma_1 = \gamma_2 = 0.5$ and the tuning parameters are calculated based on the proposed tuning relations as mentioned in eqs. (28)–(31). Proposed scheme provides lesser IAE values as provided in Table 3 computed from the process responses as shown in Figure 7 during set point tracking as well as load rejection phases compared to *i*SIMC [1] settings.

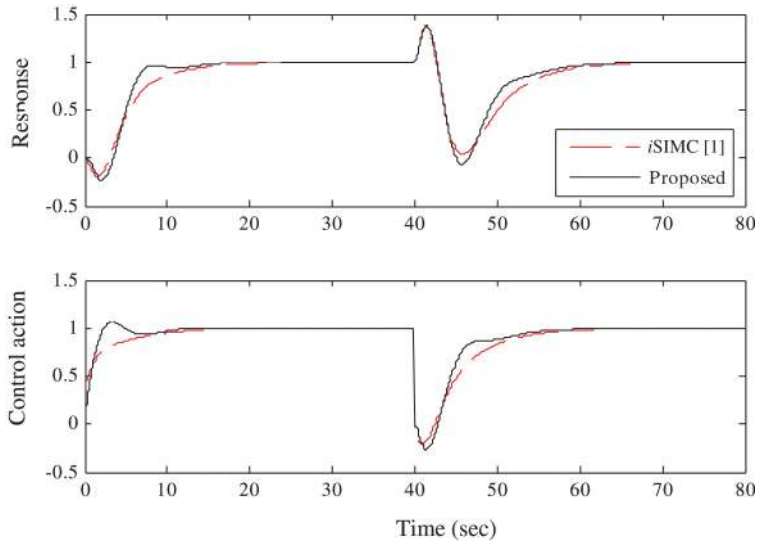

Figure 7: Closed loop responses of model II.

Model III: $\frac{(-s+1)}{(s+1)^5}e^{-2s}$

This RHP zero with time delay process model is chosen from [18]. Approximated FOPDT models based on half rule method [7] as well as our proposed technique are given by $\frac{1}{(1.5s+1)}e^{-6.5s}$ and $\frac{1}{(1.625s+1)}e^{-6.375s}$ respectively. Here, $\lambda_1 = 22.67$ and $\lambda_2 = 1.55$ with $\gamma_1 = \gamma_2 = 0.5$ and the tuning parameters are calculated based on eqs. (32)–(35). Now, closed loop response of the proposed scheme is compared with the recently published work by Grimholt and Skogestad [1] where the tuning relations are computed based on eq. (41). Like previous cases, proposed method provides lesser IAE values as provided in Table 3 computed from the process responses as shown in Figure 8 compared to *i*SIMC [1] settings.

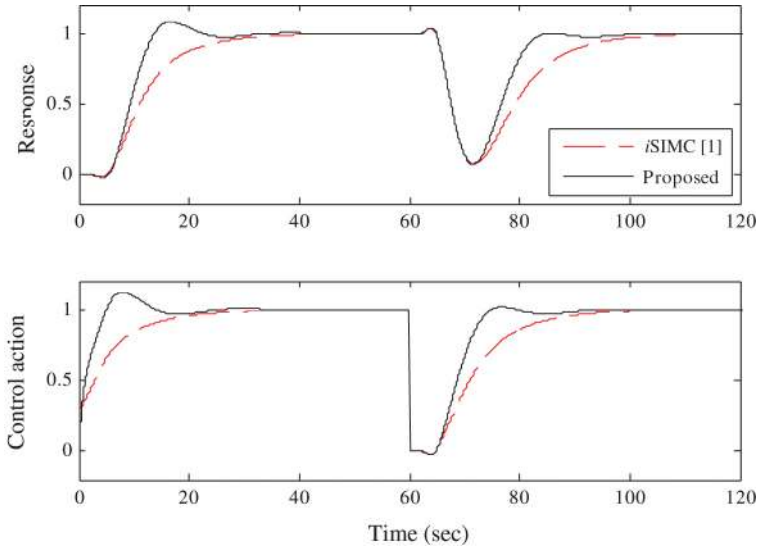

Figure 8: Closed loop responses of model III.

4.2 Real-time experimentation

Performances of the proposed scheme along with *i*SIMC tuning relations are also tested on a level control loop. It is a quad-coupled tank process manufactured by FEEDBACK [21]. In the reported experimental study only one tank (i. e. Tank 3 as shown in Figure 9(a) enclosed by dotted boundary) is chosen. During closed loop operation our goal is to maintain the water level at the desired position during set point change and load variation. Advantech PCI 1711 data acquisition (DAQ) card is used to interface between the experimental process and the PC. Sampling rate of the DAQ card is 0.1 sec. Our proposed controller along with *i*SIMC controllers are designed in PC with the help of Matlab-Simulink software. To design the proposed IMC controller, knowledge of the process model is essential.

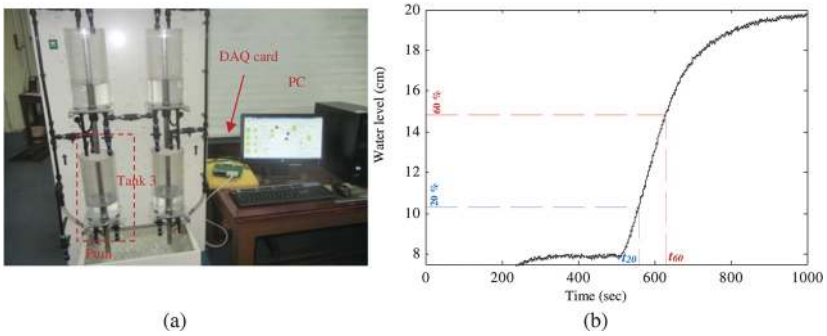

Figure 9: (a) Real-time experimental set up, and (b) PRC response from Tank 3.

To identify the model of the Tank 3, a known step input is applied to the pump at 500 sec. In this real-time experimental set up a time delay of 2.3 sec is also incorporated by introducing a delay block. The transfer function of Tank 3 is second-order as the water supply of Tank 3 coming from an upper tank which is itself a first-order process. Model of the second-order process can be identified from empirical process data [22, 23]. As a result, open loop process response is obtained as shown in Figure 9(b). Smith technique [23] can be used to identify the second-order model. To identify the tank model, t_{20} (time taken to reach 20 % of final value) and t_{60} (time taken to reach 60 % of final value) are calculated from open-loop response and t_{60}/τ is calculated from Smith chart [23]. The identified process model is given by

$$G_p(s) = \frac{11.60}{(87.5s+1)(19.27s+1)} e^{-2.3s}. \tag{42}$$

Subsequently, the approximated FOPDT models are obtained from eq. (42) using half rule and the proposed scheme which are given by $\frac{11.60}{(97.135s+1)} e^{-11.93s}$ and $\frac{11.60}{(97.665s+1)} e^{-11.404s}$ respectively. In the proposed case, tuning parameters are calculated using eqs. (28)–(31) where λ_1 and λ_2 are 40.55 and 2.78 respectively (using eq. (37)) with $\gamma_1 = \gamma_2 = 0.5$. The *i*SIMC controller is tuned using eq. (41) and all the tuning parameters are listed in Table 4. With these tuning parameters real-time closed loop performance is evaluated with the Tank 3 of the coupled tank system [21]. Once the water level of Tank 3 reaches the desired height, load disturbance is introduced at 800 sec. Responses and corresponding control action obtained from *i*SIMC tuning methodology along with the proposed technique are shown in Figure 10 and the related performance indices are listed in Table 4. All the responses along with the calculated performance indices clearly justify the superiority of the proposed IMC-PID tuning.

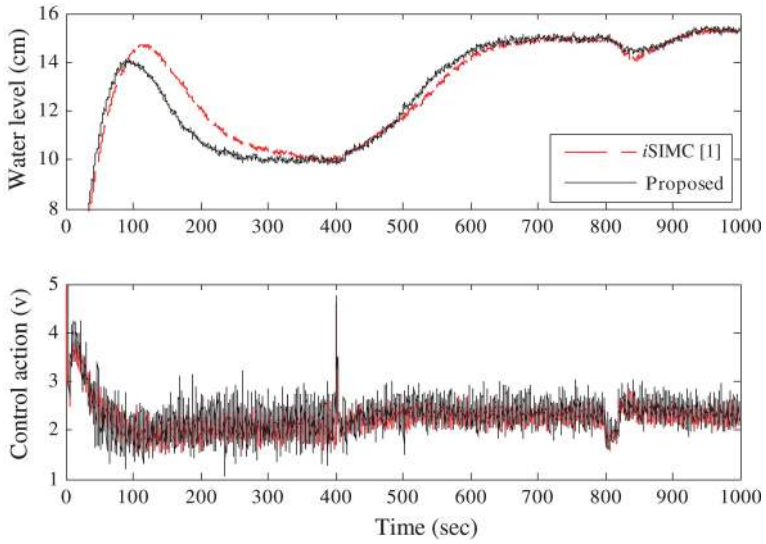

Figure 10: Responses of the proposed tuning technique along with *i*SIMC [1] settings during set point tracking and load recovery phases for real-time level control loop.

Table 4: Real-time experimental results.

Tuning	Controller parameter				Set point tracking		Load rejection	
	k_c	τ_I	τ_D	τ_F	IAE	TV	IAE	TV
*i*SIMC [1]	0.365	99.45	3.819	–	2.31×10^3	672.26	793.35	139.53
Proposed	0.648	103.36	5.387	0.773	2.23×10^3	978.71	789.26	196.15

5 Conclusion

In this work, a simple and straight forward designing of an IMC-PID controller is proposed for FOPDT process which is obtained based on a model reduction technique. To obtain the IMC-PID structure a second-order filter is also suggested with two different fractional-order time constants and an attempt is also made to adjust the fractional terms to obtain optimal behavior of the controller. Usefulness of the proposed model reduction technique and resulting IMC-PID controller is tested on well accepted higher-order models (both minimum phase and non-minimum phase) during closed loop operation in comparison with *i*SIMC tuning relations. In addition to the simulation study, effectiveness of the proposed tuning is also demonstrated on a real-time level control loop.

References

[1] Grimholt C, Skogestad S. Optimal PI and PID control of first-order plus delay processes and evaluation of the original and improved SIMC rules. J Process Control. 2018;70:36–46.
[2] Desborough LD, Miller RM. Increasing customer value of industrial control performance monitoring-Honeywell's experience. Chemical process control–VI (Tuscon, Arizona, Jan. 2001). AIChE Symp Series. 2002;326:169–89.
[3] Li M, Meng X. Design and application of PID control system of IMC. Advances in Computer Science, Environment, Ecoinformatics, and Education, Springer Series Communications in Computer and Information Science 2011;218:94–9.
[4] Rivera DE, Morari M, Skogestad S. Internal model control. 4. PID controller design. Ind Eng Chem Res. 1986;25:252–65.
[5] Chien IL. IMC–PID controller design-an extension. IFAC Proc Series. 1988;6:147–52.
[6] Morari M, Zafiriou E. Robust process control. New Jersy: Prentice- Hall, 1989.
[7] Skogestad S. Simple analytic rules for model reduction and PID controller tuning. J Process Control. 2003;13:291–309.
[8] Lee J, Cho W, Edgar TF. Simple analytic PID controller tuning rules revisited. Ind Eng Chem Res. 2014;53:5038—47.
[9] Skogestad S. Tuning for smooth PID control with acceptable disturbance rejection. Ind Eng Chem Res. 2006;45:7817–22.
[10] Astrom KJ, Panagopoulos H, Hagglund T. Design of PI controllers based on non-convex optimization. Automatica. 1998;34:585–601.

[11] Ali A, Majhi S. PI/PID controller design based on IMC and percentage overshoot specification to controller set point change. ISA Trans. 2009;48:10–5.
[12] Begum KG, Rao AS, Radhakrishnan TK. Maximum sensitivity based analytical tuning rules for PID controllers for unstable dead time processes. Chem Engg Res Design. 2016;109:593–606.
[13] Grimholt C, Skogestad S. Optimal PI-control and verification of the SIMC tuning rule. IFAC Proc Vol. 2012;45:11–22.
[14] Wang Q, Lu C, Pan W. IMC PID controller tuning for stable and unstable processes with time delay. Chem Eng Res Design. 2016;105:120–9.
[15] Saxena S, Hote YV. Simple approach to design PID controller via internal model control. Arab J Sci Eng. 2016;41:3473–89.
[16] Najafizadegan H, Merrikh-Bayat F, Jalilvand A. IMC-PID controller design based on loop shaping via LMI approach. Chem Eng Res Design. 2017;124:170–80.
[17] Shamsuzzoha M. IMC based robust PID controller tuning for disturbance rejection. J Cent South Univ. 2016;23:581–97.
[18] Shamsuzzoha M, Skogestad S. The setpoint overshoot method: A simple and fast closed-loop approach for PID tuning. J Process Control. 2010;20:1220–34.
[19] Liu T, Gao F. Industrial process identification and control design. London: Springer-Verlag, 2012.
[20] Yu CC. Autotuning of PID controllers a relay feedback approach. London: Springer-Verlag, 2006.
[21] User manual: Coupled Tank control experiments- 33-041S. East Sussex, UK: Feedback Instruments Ltd., 2010.
[22] Sundaresan KR, Krishnaswamy RR Estimation of time delay, time constant parameters in time, frequency, and laplace domains. Can J Chem Eng. 1978;56:257–62.
[23] Seborg DE, Edgar TF, Mellichamp DA. Process dynamics and control. Singapore: Wiley, 2004.